electronics

MDPI

Article

A Printed Yagi Antenna for CubeSat with Multi-Frequency Tilt Operation

Sining Liu *, Raad Raad, Panagiotis Ioannis Theoharis and Faisel Em Tubbal

School of Electrical, Computer and Telecommunications Engineering, University of Wollongong, Wollongong, NSW 2522, Australia; raad@uow.edu.au (R.R.); pit289@uowmail.edu.au (P.I.T.); faisel@uow.edu.au (F.E.T.)

* Correspondence: sl527@uowmail.edu.au

Received: 1 June 2020; Accepted: 10 June 2020; Published: 12 June 2020



Abstract: In this paper, a printed Yagi antenna with an integrated balun is proposed for CubeSat communications. The printed antenna is mechanically adjustable to realize three functional states at different operating frequencies in the L-band and S-band respectively. Three different angle deployments are proposed at 10°, 50° and 90°, so that the antenna operates at three different operating frequencies, namely 1.3 GHz (L-band), 2.4 GHz (S-band) and 3 GHz (S-band). The measured results of the fabricated antenna are well matched with the simulation, having frequencies of 2.82–3.07 GHz, 1.3–1.4 GHz and 2.38–2.57 GHz, with similar radiation patterns. The measured gain of the antenna is 8.167 dBi at 2.4 GHz, 5.278 dBi at 1.3 GHz and 6.120 dBi at 3 GHz. Keeping within the general theme of cheap off the shelf components for CubeSats, this antenna design allows the CubeSat designers to choose from three popular frequencies, through a simple angle configuration. The main contribution of this work lies with the reconfigurable frequency, relatively high gain and simplicity of design.

Keywords: antenna; CubeSat; compact antenna; integrated balun; printed antenna; reflection coefficient; Yagi antenna; Yagi-Uda antenna

1. Introduction

Conventional satellites are large, e.g., >100 kg, and cost millions of dollars to manufacture, however, CubeSats are lightweight, e.g., 1–6 kg, and provide a cost-effective way to realize space missions [1,2]. As shown in Figure 1a, the standard 1U CubeSat has dimensions of 10 cm × 10 cm × 10 cm and it can also be manufactured as 2U (10 cm × 10 cm × 20 cm), 3U (10 cm × 10 cm × 30 cm) and in other configurations [3]; see Figure 1b,c respectively. The first CubeSat mission was launched in 2003 and a steady number of CubeSats have been launched every year since 2013 when commercial applications joined the field [4]. To date, several CubeSats have been designed, launched and operated successfully at low earth orbit (LEO); examples include CanX-1, CUTE-1, and AUU [5].

Due to the CubeSat's limited size, weight and power budget, designing antennas for the CubeSat platform is a challenging task. This means that any antenna design needs to comply with the size and the mass restrictions of CubeSats, to provide more space for solar cells and meet operating frequency requirements and mission objectives. Moreover, with the growth of small satellite technologies, CubeSats are being endowed with more challenging missions that require a high data rate, which must be supported by high gain directional antennas.

Various proposed high gain antenna designs for CubeSat applications are large in size and require deployment mechanisms. For example, in Reference [6], the authors proposed a deployable dipole antenna

using a curved bi-stable composite tape-spring technique that can be stowed on CubeSat, but deploy to several meters long. Designs of deployable helical UHF antennas are presented in [7,8]. They provide high gains, e.g., >8 dB, however, their main limitation is their large size, e.g., >20 cm in length when deployed, and occupy significant volume on the CubeSat when folded, which in turn limits the area for solar cells and affects the operational lifetime

Planar antennas have a low profile and do not require deployment and hence reduce the cost if properly designed. For example, in Reference [9,10], the authors presented two patch antenna designs for CubeSat. These antenna designs are small and do not require deployment and provide gains of only 4.8 dBi in [9] and 5.3 dBi in [10]. The design of a patch antenna with a feeding network in [11] has achieved a small size of 23 mm × 20 mm, however, its total gain is low, e.g., 4 dBi. Reference [12] presented a dual band planar antenna with compact structure and shows 5.4 dBi gain. A patch antenna integrated with a solar panel was proposed for CubeSat applications in [13], which can achieve a relatively higher gain of 5.96 dBi. However, with a low profile, the highest gain of the mentioned designs is no larger than 6 dBi.

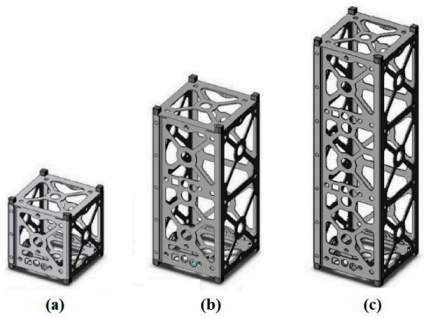

Figure 1. Cube Satellite: (**a**) 1U; (**b**) 2U; (**c**) 3U [11].

Recently, a number of compact Yagi-like antenna designs, with flexibility for a wide range of applications, were proposed. We mention these antennas for completeness of work, while none of them was specifically designed for CubeSat. They are general in nature and have not been tested on a CubeSat, and hence, their performance is not clear when combined with a cubic metallic body. We also note that none of the mentioned designs employ the mechanical lift mechanism that we are proposing to use in this paper. These state of the art antennas are further compared to the proposal in this paper in Table 1, which appears later in the paper, after the results section.

The state of the art antennas used various feeding methods and balun techniques. An X-band coplanar waveguide (CPW) fed broadband a Yagi antenna was presented in [14]. It has no extra balun component and achieved a total gain of 7.4 dBi in the X-band. A microstrip-to-coplanar (CPS) strip transition line method for quasi-Yagi was proposed in [15,16]. The quasi-Yagi antenna presented in [15] was built on 3C Rogers substrate (RO400) and achieved a total gain of 4 dBi, while the quasi-Yagi antenna in [16] was built on two-layer substrate made by Duroid 5880 and Rohacell foam and reported a total gain of 6.5 dBi. Moreover, in Reference [17], the authors proposed a printed Yagi antenna fed by folded dipole feed and tapered balun. It provided a total gain of 7 dBi, but with six directors and relatively large dimensions. Another printed Yagi antenna was presented in [18], where it was built on a FR4 substrate and fed by a monopole microstrip (MS) line. It also presents improved performance by tapering the feeding line. The proposed antenna achieves gains of 4.1 dBi (monopole MS feed line) and 4.65 dBi (tapering the feeding line). Moreover, [19] proposed two different configurations based on compact Yagi antenna on FR4 substrate fed by rectangular strip feed and tapered strip feed, which show gains of 6.3 dBi and 6.4 dBi respectively. It can be seen that the largest gain among the prementioned designs is 7.4 dBi in [14], achieved on X-band, while being 7 dBi on S-band in [17], but the design is extended to six directors and is relatively long in size.

Table 1. Frequency, bandwidth and gain for all states and compared with the state of art designs.

Antenna	Remark	Operating Band (GHz)		−10 dB Bandwidth (MHz (%))		Operating Frequency (GHz)	Return Loss (dB)		Gain (dBi)		Balun/Feed Structure	Size (mm)
		Simu	Meas	Simu	Meas		Simu	Meas	Simu	Meas		
Band 1	$A = 10°$	2.88–3.19	2.82–3.07	310 (10.2)	250 (8.4)	3.0	−16.2	−24.2	9.03	8.17	Tapered balun/Single side printed	100 × 98
Band 2	$A = 50°$	1.23–1.38	1.30–1.40	150 (11.4)	100 (7.4)	1.3	−23.8	−14.5	5.47	5.28		
Band 3	$A = 90°$	2.34–2.52	2.38–2.57	180 (7.4)	190 (7.6)	2.4	−18.4	−18.5	7.09	6.12		
[14]	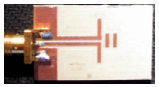	8–12		44%		10.0	−24		3.4–7.4		CPW	19.2 × 29
[15]	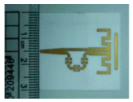	5–7		33%		5.6	−14		4.1–4.5		CPS	30 × 42.5
[16]	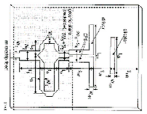	9.5–11.6		17%		10.9	−22		6.5		CPS	15 × 18
[17]	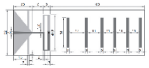	2.31–2.5		7.7%		2.45	−23		7.5 (6 directors)		Folded dipole/Tapered balun	52 × 143
[18]	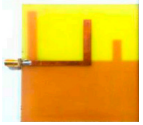	1.7–2.1		47.6%		1.8	−18		4.1		MS line	76 × 86
	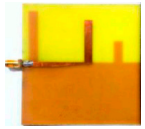	1.5–2.53		53.5%		2.2	−15		4.65		Tapered MS line	
[19]	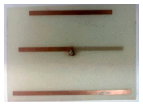	1.2–1.4		15.4%		1.3	−28		6.3		Rectangular strip	85 × 112
		1.18–1.41		18.6%		1.29	−37		6.4		Tapered strip	85 × 102

To address the aforementioned limitations between antenna size and performance for CubeSat applications, we propose a printed Yagi antenna with a tapered balun integrated on the substrate. As shown in Figure 2, reflector, driven and director elements are printed on FR4 substrate and form a Yagi shape. FR4 dielectric is adopted in this antenna design, as it has been widely used, both in PCBs and antennas on low earth orbit (LEO) CubeSat missions, providing a low cost alternative to other expensive low loss dielectrics [20,21]. The operating frequency of the proposed antenna can be adjusted so that the antenna operates at L-band and S-band by rotating the antenna around its x-axis. The main contributions of this paper are the adaptive frequency operation achieved by adjusting the angle between the antenna and satellite, and the high achieved gains at different angles and frequency bands. Here, we note that the deployed angle maybe be fixed. For example, we can deploy at an angle of 50° for L-band operation. It is also possible to build a deployment mechanism that will allow multi-angle operations and hence different frequencies, giving the CubeSat extra mission flexibility by being able to operate at different frequencies when required.

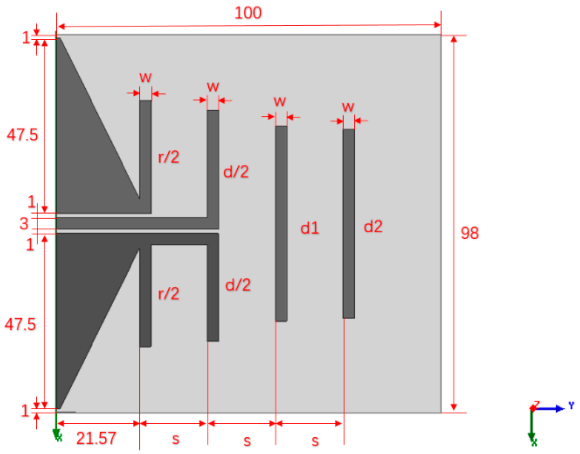

Figure 2. Layout of the printed Yagi antenna (units in mm).

2. Design of Printed Yagi Antenna on CubeSat

2.1. Dimensions of Printed Yagi Antenna

The proposed Yagi antenna is printed on an FR4 substrate, with a dielectric constant of 4.4 and a loss tangent of 0.02, and has four elements, including the reflector, driven element and two directors; see Figure 2. The 50 Ω impedance matching of the antenna is achieved through a tapered balun integrated with the printed antenna. The antenna has a total size of 100 mm × 98 mm, which is smaller than the CubeSat surface. The optimal parameter values of the proposed antenna are as follows: r = 58.8 mm, d = 58.8 mm, d1 = 50.5 mm, d2 = 48.8 mm, w = 3 mm, s = 14.6 mm. The length of the driven element is chosen to be close to the half-wavelength of 2.5 GHz; the lengths of directors are 0.43λ, 0.415λ and 0.4λ, so that the antenna can be optimized to operate at S-band without considering the interaction of the CubeSat that is made by aluminum. The spacing between each element is between 0.1λ to 0.2λ. The gaps between the negative tapered parts and positive feeding element in the central are both 1 mm, and the tapered ground is 1 mm away from the edge of substrate for both sides. All the printed elements are on the upper layer of the substrate.

2.2. CubeSat-Antenna Configuration

Before launching the CubeSat, the antenna is required to be stowed, as shown in Figure 3a. The deployed functional geometry of the proposed antenna is shown in Figure 3b, that involves a rotation by an angle A around the antenna's x-axis. In practice, the deployment of the antenna can be realized by a hold and release system, where the antenna is held within a stowed structure and push to the functional structure by a deploying force when needed. This force can be created by a mechanical spring that compresses itself when the antenna is stowed and back to original size when lifting the antenna. This allows for a single angle deployment, hence, as will be seen from the results, at 90°, an operating frequency of 2.4 GHz is realized. If more functionality is required, as mentioned earlier, a more elaborate system can be installed, that allows multiple lift angles. In order to control the variable status of angle A with a smooth steerable change, a linear actuator controlled by a DC motor can be used.

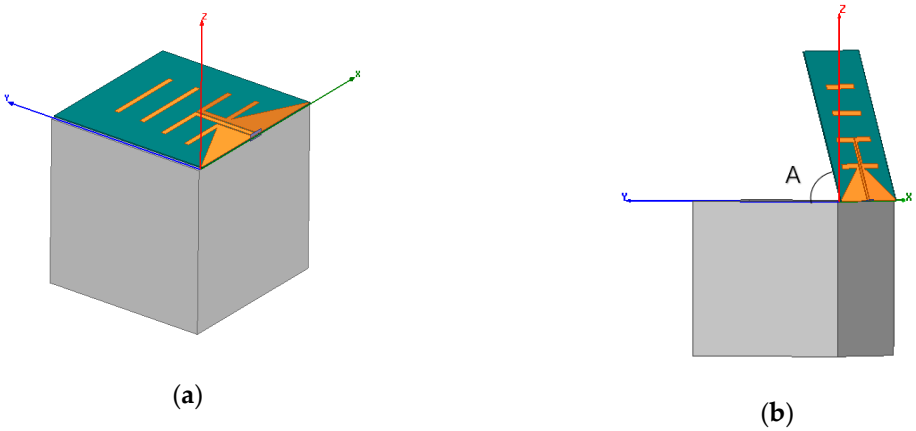

(**a**) (**b**)

Figure 3. Proposed antenna on CubeSat in: (**a**) Stowed structure and (**b**) Functional structure.

By changing angle A, the antenna can provide an adaptive frequency operation. For instance, when angle A equals 90°, the antenna resonates at 2.4 GHz, as the CubeSat body has little interaction with the antenna. When A is equal to 10° or 50°, the antenna gets closer to the CubeSat top surface, hence, the coupling between the antenna and CubeSat becomes stronger. Furthermore, exploiting the coupling between the antenna and the CubeSat, different resonant frequencies are generated at L-band and S-band, giving rise to multi-frequency antenna operation. However, one of the main challenges would be to precisely point the antenna at 10°, 50° and 90°, as the resonant behavior is affected by accuracy of the pointing angle. Apart from that, the gain and −10 dB bandwidth of the antenna must be maintained within reasonable levels at different operating frequency modes obtained at different pointing angles A.

3. Simulation and Measurement Results

3.1. Antenna Fabrication and Experiment Setup

A fabrication was completed according to the proposed Yagi model. As shown in Figure 4, all elements are printed on FR4 substrate, with a dielectric constant of 4.4 and a thickness of 0.6 mm. A SubMiniature version A (SMA) coaxial connector was used to feed the antenna through the central feeding line and grounded on the tapered balun. The antenna is placed on the body of a 10 cm × 10 cm × 10 cm aluminum box. Figure 4 shows the fabricated antenna with three different configurations at three different angles.

A high frequency simulator structure (HFSS) [22] is used to simulate the proposed Yagi antenna. The measurements of the reflection coefficients of the fabricated Yagi antenna were conducted by using

Keysight's E5063A Vector Network Analyzer (VNA). The measurement of the antenna radiation pattern was conducted in a far-field anechoic chamber located in the Laboratory at the University of Wollongong, cancelling any interference from the outside and minimizing any unwanted reflections, hence ensuring that the measurement environment is close to the HFSS free space simulation environment.

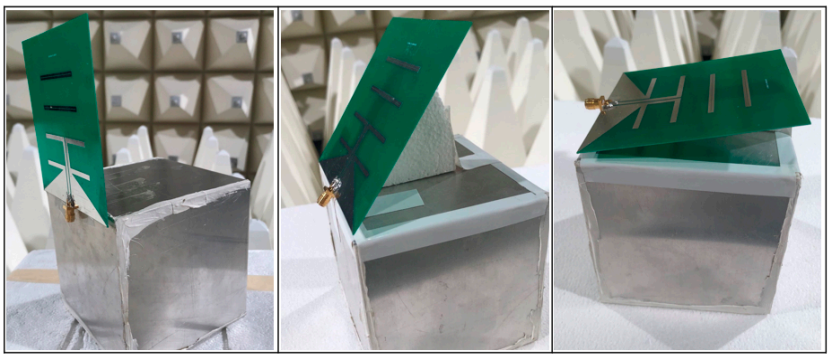

Figure 4. Fabricated antenna on 1U Cube with various lift angle.

3.2. Reflection Coefficient

Figure 5 compares the simulated and measured reflection coefficients of the proposed antenna when it is placed on top of the 1U Cube Model. The proposed antenna was measured at three different angles, e.g., A = 10°, A = 50°, A = 90°. When A = 10°, the antenna resonates at 3 GHz, see Figure 5a. The measured −10 dB bandwidth is 250 MHz, ranging from 2.82 GHz to 3.07 GHz, with a small reflection coefficient of −24.16. As shown in Figure 5b, when A = 50°, the antenna provides a measured reflection coefficient (S11) of −14.49 dB at 1.3 GHz, with −10 dB bandwidth of 100 MHz (1.3–1.4 GHz). Figure 5c shows that, at A = 90°, the antenna provides a good agreement between simulation and measurement as the antenna operates at S-band (e.g., 2.45 GHz). The antenna achieved a measured reflection coefficient (S11) of −18.47 dB at 2.45 GHz, with −10 dB bandwidth of 190 MHz (2.38–2.57 GHz). Details of the comparisons of frequency, bandwidth, reflection coefficient, gain, feed method and antenna size between the proposed antenna and some other printed Yagi antenna designs are listed in Table 1.

3.3. Radiation Pattern

Figure 6 shows the 3D polar plot of proposed antenna at 2.4 GHz when A = 90°. The simulated and measured radiation patterns at three different frequency bands on the plane ϕ = 90° and θ = 90° are shown in Figure 7. The measured patterns show similar shapes, with simulation results and matched maximum radiation direction. In plane ϕ = 90°, the directions of radiation slightly tilt to the left by 35° when the angle A is decreased from 90° to 50° and 10°, while the direction of plane θ = 90° remains unchanged in three bands. In general, the antenna shows directional behavior on both plane when A = 90° and 50°. Meanwhile, when A = 10°, the measured radiation pattern is closer to unidirectional on θ = 90° and obvious directional on ϕ = 90°. There are good agreements between simulation and measurement for all three states. The maximum gains for each frequency bands from simulation and measurement are presented in Table 1.

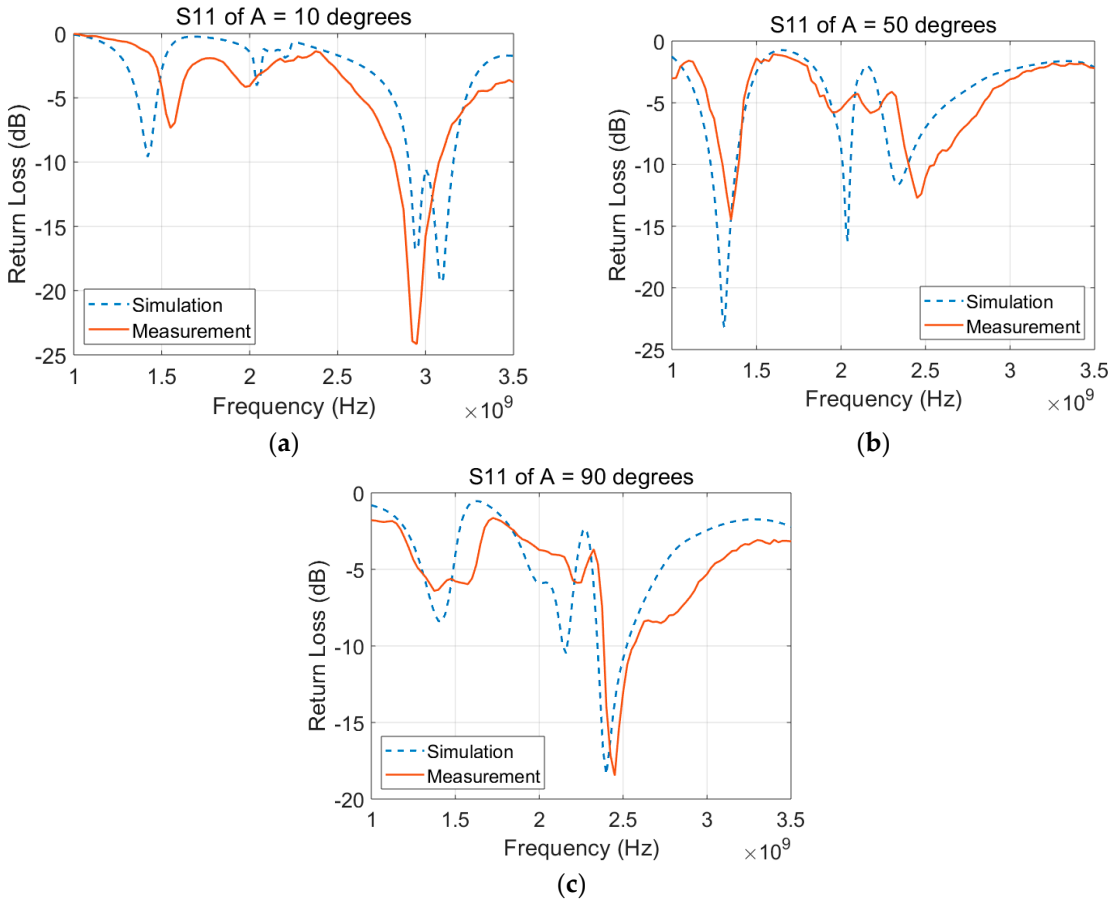

Figure 5. Reflection Coefficients of Simulation and Measurement. (**a**) A = 10°, (**b**) A = 50°, (**c**) A = 90°.

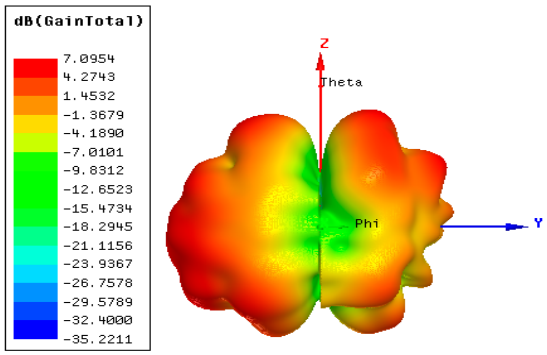

Figure 6. 3D polar plot at 2.4 GHz when A = 90°.

Compared with other printed Yagi antenna designs, e.g., those listed in Table 1, our proposed antenna provides the highest gain at angle $A = 10°$, that is 8.167 dBi in measurement, however, its bandwidth is narrower. Reference [17] shows higher value of gain than other designs, but the size of this antenna is 43 mm longer than our proposed structure. Thus, besides the adaptive frequency operation, the proposed antenna with tapered balun provides good gain performance in terms of higher gain, and a low reflection coefficient based on the feasible size for CubeSat applications.

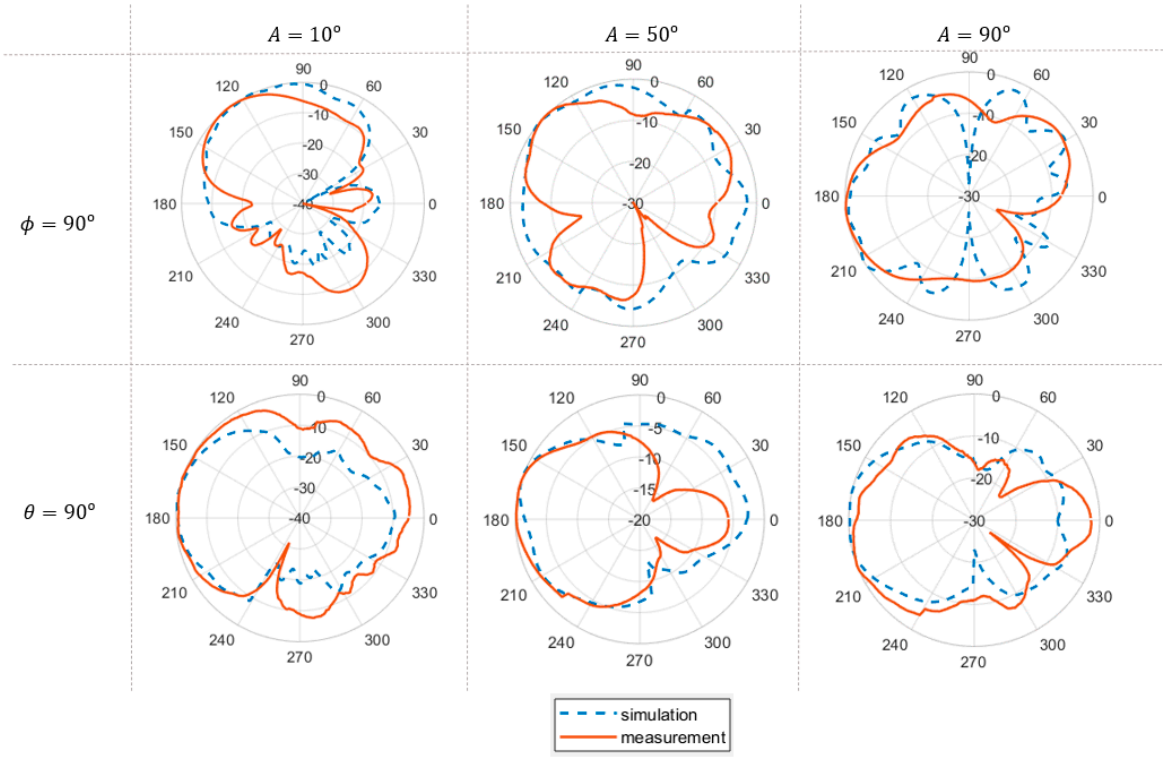

Figure 7. Radiation patterns for plane ϕ = 90° and θ = 90° of simulation and measurement.

4. Comparison and Discussion

Table 1 presents a comparison of our proposed antenna design, with reported Yagi-like antenna designs presented in the literature. A photo of each mentioned design is shown in the second column. There are two antennas designed for X-band in [14,16], and one design in [15] for C-band. Reference [17,19] operate on similar frequency bands with the proposed antenna, which is for 1.2–1.4 GHz in the L-band and 2.3–2.5 GHz in the S-band. Most of the listed antenna designs in Table 1 provide wide bandwidths, e.g., >33%, however, the antenna designs presented in [16,19] provide small bandwidths of 17% and 18%, respectively. Moreover, compared to all the antenna designs presented in Table 1, the one in [18] provides the widest bandwidth of 53.5% and the one in [17] provides the smallest bandwidth, at only 7.7%. We noted that tapering a MS feeding line can help to improve the bandwidth, which is proved by [18,19], while tapered baluns provide narrower bandwidth than CPW and CPS. In terms of the reflection coefficient, all presented antenna designs provide a relatively small reflection coefficient. Our proposed antenna provides a smaller reflection coefficient of −24.2 dB (e.g., band 1), as compared to designs in [14–18]. Compared to all antenna designs listed in Table 1, our proposed antenna provides the highest gain of 8.17 dB (band 1). In addition, the sizes of antennas are presented in the last column. In general, a higher frequency can lead to a smaller antenna size. Antennas in Reference [14–16] are smaller than others, as they are designed for the C-band and the X-band. Compared with antenna on L-band and S-band in [17,19], the proposed antenna shows a reasonable size, that is smaller than the CubeSat surface. Although Reference [18] provides a smaller size of only 76 mm × 86 mm, the gain of this design is less than 5 dBi.

5. Conclusions

A compact design of a Yagi antenna that was printed on FR4 substrate with an integrated balun is presented in this paper. The proposed antenna provides an adaptive frequency operation in the L-band

(1.3–1.4 GHz) and S-band (2.38–2.54 GHz and 2.82–3.08 GHz), using a simple deployment mechanism. However, the pointing accuracy of the antenna defined by angle A is of great importance, as it determines the operating frequency band of the proposed design. The main advantages of the proposed antenna are the low manufacturing cost, and its capability for multi frequency operation while maintaining high gain at the different frequency bands. Moreover the proposed antenna present a compact volume and low profile, making it a suitable candidate for CubeSat missions. The antenna design achieves a total measured gain of 8.16 dBi, 5.78 dBi, and 6.12 dBi at 3 GHz, 1.3 GHz and 2.4 GHz respectively. It also achieves −10 dB bandwidths of 250 MHz at 3 GHz, 100 MHz at 1.3 GHz and 190 MHz at 2.4 GHz. The measurements of the fabricated antenna are in good agreement with the simulation and proved the reconfiguration technique of the design.

Author Contributions: Conceptualization, S.L. and R.R.; methodology, S.L. and P.I.T.; software, S.L. and F.E.T.; validation, S.L. R.R. and P.I.T.; formal analysis, R.R.; investigation, P.I.T.; resources, S.L. and R.R.; data curation, S.L and P.I.T.; writing—original draft preparation, S.L.; writing—review and editing, R.R., P.I.T. and F.E.T.; supervision, R.R.; project administration, S.L. All authors have read and agreed to the published version of the manuscript.

Funding: This research received no external funding.

Acknowledgments: The authors thank Shansong Huang for his help in writing, investigating and using software.

Conflicts of Interest: The authors declare no conflict of interest.

References

1. Tubbal, F.E.; Raad, R.; Chin, K.; Butters, B.; Matekovits, L.; Dassano, G. A high gain s-band CPW-fed slot antenna for cubesat. *Ann. Telecommun.* **2019**, *74*, 223–237. [CrossRef]
2. Heidt, H.; Puig-Suari, J.; Moore, A.; Nakasuka, S.; Twiggs, R. CubeSat: A new generation of picosatellite for education and industry low-cost space experimentation. In Proceedings of the 14th Annual AIAA/USU Conference on Small Satellites, Logan, UT, USA, August 2000; Available online: https://digitalcommons.usu.edu/smallsat/2000/All2000/32/ (accessed on 6 May 2020).
3. Tubbal, F.; Raad, R.; Chin, K.-W. A Survey and Study of Planar Antennas for Pico-Satellites. *IEEE Access* **2015**, *3*, 2590–2612. [CrossRef]
4. Swartwout, M. The first one hundred cubesats: A statistical look. *J. Small Satell.* **2013**, *2*, 213–233.
5. Klofas, B.; Anderson, J.; Leveque, K. A survey of cubesat communication systems. In Proceedings of the 5th Annual CubeSat Developers' Workshop, San Luis Obispo, CA, USA, 9–11 April 2008; pp. 1–36.
6. Murphey, T.; Jeon, S.; Biskner, A.; Sanford, G. Deployable booms and antennas using bi-stable tape-springs. In Proceedings of the 24th Annual AIAA/USU Conference on Small Satellites, Logan, UT, USA, August 2010; Available online: https://digitalcommons.usu.edu/smallsat/2010/all2010/58/ (accessed on 7 May 2020).
7. Ochoa, D.; Hummer, K.; Ciffone, M. Deployable Helical Antenna for nano-Satellites. In Proceedings of the 28th Annual AIAA/USU Conference on Small Satellites, Logan, UT, USA, August 2014; Available online: https://digitalcommons.usu.edu/smallsat/2014/AdvTechComm/4/ (accessed on 10 May 2020).
8. Muri, P.; Challa, O.; McNair, J. Enhancing small satellite communication through effective antenna system design. In Proceedings of the 2010 - Milcom 2010 Military Communications Conference, San Jose, CA, USA, 31 October–3 November 2010; pp. 347–352.
9. Tubbal, F.; Raad, R.; Chin, K.-W.; Butters, B. S-band shorted patch antenna for inter pico satellite communications. In Proceedings of the 2014 8th International Conference on Telecommunication Systems Services and Applications (TSSA), Kuta, Indonesia, 23–24 October 2014; pp. 1–4.
10. Tubbal, F.; Raad, R.; Chin, K.W.; Butters, B. S-band Planar Antennas for a CubeSat. *Int. J. Electr. Eng. Informatics* **2015**, *7*, 559–568. [CrossRef]
11. Veljovic, M.; Skrivervik, A.K. Aperture-Coupled Low-Profile Wideband Patch Antennas for CubeSat. *IEEE Trans. Antennas Propag.* **2019**, *67*, 3439–3444. [CrossRef]

12. Yao, Y.; Liao, S.; Wang, J.; Xue, K.; Balfour, E.A.; Luo, Y. A New Patch Antenna for CubeSat: Dual feed, L/S dual-band stacked, and circularly polarized. *IEEE Antennas Propag. Mag.* **2016**, *58*, 1. [CrossRef]
13. Jones, T.R.; Grey, J.P.; Daneshmand, M. Solar Panel Integrated Circular Polarized Aperture-Coupled Patch Antenna for CubeSat Applications. *IEEE Antennas Wirel. Propag. Lett.* **2018**, *17*, 1895–1899. [CrossRef]
14. Kan, H.K.; Waterhouse, R.B.; Abbosh, A.; Bialkowski, M.E. Simple Broadband Planar CPW-Fed Quasi-Yagi Antenna. *IEEE Antennas Wirel. Propag. Lett.* **2007**, *6*, 18–20. [CrossRef]
15. Ma, T.-G.; Wang, C.-W.; Hua, R.-C.; Tsai, J.-W. A Modified Quasi-Yagi Antenna with a New Compact Microstrip-to-Coplanar Strip Transition Using Artificial Transmission Lines. *IEEE Trans. Antennas Propag.* **2009**, *57*, 2469–2474. [CrossRef]
16. Qian, Y.; Deal, W.; Kaneda, N.; Itoh, T. Microstrip-fed quasi-Yagi antenna with broadband characteristics. *Electron. Lett.* **1998**, *34*, 2194. [CrossRef]
17. Farran, M.; Capobianco, A.-D.; Modotto, D.; Locatelli, A.; Midrio, M.; Ferrari, V.; Boscolo, S. Compact quasi-Yagi antenna with folded dipole fed by tapered integrated balun. *Electron. Lett.* **2016**, *52*, 789–790. [CrossRef]
18. Chaudhari, A.D.; Ray, K.P. Printed broadband Quasi-Yagi antenna with monopole elements. *IET Microwaves Antennas Propag.* **2020**, *14*, 468–473. [CrossRef]
19. Kumar, H.; Kumar, G. Compact planar Yagi-Uda antenna with improved characteristics. In Proceedings of the 2017 11th European Conference on Antennas and Propagation (EUCAP), Paris, France, 19–24 March 2017; pp. 2008–2012.
20. Triana, J.S.; Bautista, S.; González, F.A.D. Identification of Design Considerations for Small Satellite Remote Sensing Systems in Low Earth Orbit. *J. Aerosp. Technol. Manag.* **2015**, *7*, 121–134. [CrossRef]
21. Rodriguez-Osorio, R.M.; Ramírez, E.F. A Hands-On Education Project: Antenna Design for Inter-CubeSat Communications [Education Column]. *IEEE Antennas Propag. Mag.* **2012**, *54*, 211–224. [CrossRef]
22. High Frequency Simulator Structure. Available online: http://www.ansys.com/ (accessed on 17 December 2019).



© 2020 by the authors. Licensee MDPI, Basel, Switzerland. This article is an open access article distributed under the terms and conditions of the Creative Commons Attribution (CC BY) license (http://creativecommons.org/licenses/by/4.0/).